LBL-37795
UC-401

A Multi-channel Monolithic Ge Detector System for Fluorescence X-ray Absorption Spectroscopy

J.J. Bucher, P.G. Allen, N.M. Edelstein, and D.K. Shuh

Chemical Sciences Division
Ernest Orlando Lawrence Berkeley National Laboratory
University of California
Berkeley, California 94720

N.W. Madden, C. Cork, P. Luke, D. Pehl, and D. Malone

Engineering Division
Ernest Orlando Lawrence Berkeley National Laboratory
University of California
Berkeley, California 94720

March 1995

This work was supported by the Director, Office of Energy Research, Office of Basic Energy Sciences, Chemical Sciences Division, of the U.S. Department of Energy under Contract No. DE-AC03-76SF00098. This work was performed in part at SSRL which is funded by the Department of Energy, Office of Basic Energy Sciences, Chemical Sciences Division.

A Multi-channel Monolithic Ge Detector System for Fluorescence X-ray Absorption Spectroscopy

J. J. Bucher, P. G. Allen, N. M. Edelstein, and D. K. Shuh

Chemical Sciences Division, Lawrence Berkeley National Laboratory, Berkeley, CA 94720

N. W. Madden, C. Cork, P. Luke, D. Pehl, and D. Malone

Engineering Division, Lawrence Berkeley National Laboratory, Berkeley, CA 94720

Keywords: detector, fluorescence, synchrotron, x-ray absorption spectroscopy

SRI '95 Submission: A06

ABSTRACT

The construction and performance characteristics of a monolithic quad-pixel Ge detector designed specifically for fluorescence x-ray absorption spectroscopy (XAS) at synchrotron radiation sources is described. The detector semiconductor element has an active surface area of 4.0 cm^2 which is electrically separated into four 1.0 cm^2 pixels, with little interfacial dead volume. The spatial response of the array demonstrates that cross-talk between adjacent pixels is less than 10% for 5.9 keV photons that fall within 0.5 mm of the pixel boundaries. The detector electronics system utilizes pre-amplifiers built at LBNL with commercial Tennelec Model TC 244 amplifiers. Employing an ^{55}Fe test source (Mn K_α, 5.9 keV), energy resolution of better than 200 eV is achieved with a 4 μsec peaking time. At 0.5 μsec peaking time, pulse pileup results in a 75% throughput efficiency for an incoming count rate of 100 kHz. Initial XAS fluorescence measurements at the beamline 4 wiggler end stations at SSRL show that the detector system has several advantages over commercially available x-ray spectrometers for low-concentration counting applications.

I. INTRODUCTION

The continued development and application of fluorescence detection techniques is essential for x-ray absorption spectroscopy (XAS) investigations of low concentration species and for systems in which there is severe matrix scattering.[1-5] This is especially important for environmentally-relevant systems since much of the chemistry and physics of environmental concern occur in aqueous solutions at sub-millimolar concentrations or in systems that have matrices which strongly scatter. New third generation synchrotron radiation (SR) sources, as well as existing insertion device beamlines, have photon fluxes that give signal intensities that cannot be fully utilized by existing detector systems.

The present state-of-the-art commercial XAS fluorescence detectors consist of thirteen element solid state Ge arrays with pulse processing electronics that discriminate fluorescent photons from a large background of scattered radiation.[2] While the signal to background of these devices offers a significant improvement over previous and alternative detection schemes, the acquisition of useful data on species at sub-millimolar concentrations is frequently limited by fluorescent photon statistics. Maximum attainable count rates are limited by saturation effects and ultimate detection limits are hampered by efficiency and stability.[1] However, recent improvements have increased the maximum count rate per channel available.[3] There are also several efforts currently underway to increase the number of channels and fabrication of 100 element arrays of Si or HgI_2.[4-5] Generally, Si detectors cover an energy range up to 20 keV, while Ge detectors extend this range to ~100 keV as a result of its higher photopeak cross-section. HgI_2 has been considered as an alternative to the low temperature (77 K) Si and Ge devices since it operates at near room temperature.[5] In contrast to the aforementioned total count rate considerations, low level counting applications in matrices that strongly scatter depend on detector element efficiency and stability of the detector electronics to provide noise free fluorescence signals.

The concept of utilizing a continuous four pixel semiconductor element was proposed as a novel solution to specialized experimental requirements. The detector has been specifically

designed for use at synchrotron radiation (SR) general user facilities to perform XAS measurements and to minimize the effects associated with a user facility environment. Herein, the initial performance characteristics of the new monolithic quad-pixel fluorescence detector are described.

II. DETECTOR SYSTEM DESIGN

The quad-pixel fluorescence detector semiconductor element consists of a monolithic high-purity 4.0 cm^2 Ge crystal that is divided electrically into four 1.0 cm^2 pixel elements solely by careful placement of the signal contacts. The detector operates with a bias of -600 V and at liquid nitrogen (77 K) temperature. A schematic of the detector element is presented in Fig. 1. The thickness of the Ge element, 6 mm, was optimized for detection of fluorescent photons in the energy range of 5-45 keV. The detector was designed to specifically minimize the effects of the inherently noisy environment that exists at SR user facilities by incorporating a high degree of mechanical and electrical stability. As an example, the experimental x-ray hutches at SSRL employ a stepping motor-driven experimental platform that induces microphonics in sensitive fluorescence detectors.[6] The detector was constructed utilizing the same mechanical stability technologies used in mounting x-ray detectors for the U. S. space programs, that must withstand vigorous rocket launches. This ruggedness is particularly helpful since the detector is shipped routinely by surface transportation to SSRL. The detector element operates under a nearly static vacuum except for a small amount of molecular sieve. The spectrometer is anticipated to require a rigorous pump-out approximately every two years. The Ge detector element is situated in the barrel of the spectrometer behind a 0.004-inch Be entrance window and a high purity 0.001-inch Be isolation window. The first Be window provides a mechanically protective barrier and vacuum secondary whereas the inner window is a thermal radiation shield and the vacuum primary. The thickness of the Be windows were selected for this particular application. The detector incorporates a vertical seven-liter liquid nitrogen Dewar hat provides cooling for more than 72 hours. The detector assembly is mounted on a high precision manual laboratory jack

affixed to an adapter plate that is in turn mounted on a remotely controlled stepper motor-driven translator stage. This combination adjustment permits both remote and center positioning of the detector with respect to the x-ray beam for optimizing count rates in each pixel element while the sample is under irradiation. The entire detector stage positioning assembly has been optically indicated for ease of alignment during beamline setup procedures.

The current configuration of the detector system electronics, excluding the pre-amplifiers, utilizes four independent channels of standard, commercially available pulse processing circuitry. The four LBNL pre-amplifiers are barrel mounted and each has a selected a low-noise field effect transistor (FET) as the first amplifying element. The FET's, whose mounts are cooled to liquid nitrogen temperature, are maintained at optimal operational temperature (~125 K) by local heaters. Pulse processing, including shaping and normal pileup rejection, is accomplished with Tennelec Model TC 244 amplifiers. The amplifier provides an incoming count rate (ICR) signal which can be used to monitor and later correct the fluorescence response for detector dead time. The output from the amplifiers is passed to individual Tennelec Model TC 451 single channel analyzer (SCA) timing discriminators. The SCA windows are monitored and set by use of an 8192 channel Oxford-Nucleus PCA II pulse height analysis (PHA) board resident in a 486 microprocessor-based computer. The windowed SCA output is terminated and filtered to remove any electrical noise with less than a 1 MHz bandwidth. The multiple SCA outputs are summed and sent to the standard SSRL data acquisition hardware via connection to a Kinetic Systems hex counter. The individual ICR and SCA signals from each pixel are also sent to hex counters and recorded for later use. The detector electronic modules are contained in two NIM bins mounted in a half-height electronics rack which is powered through an isolation transformer.

III. RESULTS AND DISCUSSION

The detector system pulse processing efficiency has been experimentally determined as a function of pulse peaking time (T_p). Figures 2 and 3 show plots of the processed SCA output versus ICR using photons from collimated ^{55}Fe (Mn K lines, ca. 5.9 keV) and ^{238}Pu (U L lines, ca. 13.6, 17.2, and 20.2 keV) sealed sources mounted on a precision XYZ translation stage, respectively. The ICR level was varied by adjusting the source-to-detector distance. The detector performance with the ^{238}Pu source is particularly germane for the intended application, study of actinide L_{III} edge systems, since many of the fluorescence lines occur at high energies (>10 keV). Pulse pileup results in a 75% throughput efficiency for an incoming count rate of 100 kHz at 0.5 μsec peaking time, per pixel. These measurements (done for a single pixel) show that the overall throughput characteristics of the quad-pixel detector is comparable to that of existing commercial multi-element detectors. Longer peaking times result in a decrease in the maximum throughput as anticipated. Dead time corrections will permit operation of the detector with ICR rates of up to 150 kHz.

The detector system resolution was measured as a function of T_p using the same ^{55}Fe and ^{238}Pu sealed sources. Resolution has been defined as the FWHM of an x-ray line observed in the output of the PHA as per standard convention. At 5.9 keV, the resolution for a single pixel ranges from 200 eV (T_p=4 μs) to 410 eV (T_p=0.5 μs). The resolution broadens slightly from 260 eV (T_p=4 μs) to 430 eV (T_p=0.5 μs) at higher energies using the ^{238}Pu source.

The extent to which the charge collection of individual pixels is electrically separated was measured by scanning a 0.1 mm diameter beam from a ^{55}Fe source mounted perpendicular to the pixel surface. The collimator was placed about 2 mm from the detector with the sealed source directly behind the 6 mm thick collimator. For example, the source was scanned from pixel 2 to pixel 1 and horizontally from pixel 2 to pixel 3 (see Fig. 1). The cross-talk between pixels was also measured with 60 keV photons from a collimated ^{241}Am source since there is interest in using the detector in its existing configuration to investigate higher energy K edges of high Z elements. Inspection of the resulting map of the detector response (SCA output versus position)

shown in Fig. 4 demonstrates that cross-talk between adjacent pixels is less than 10% for photons that fall within 0.5 mm of the pixel borders.

There is in principle no inactive portion of the array since this detector is based on a continuous monolithic design. Photons that impinge within the border regions are counted regardless of which pixel collects the charge. However, a close examination of the SCA output using a pulse height analyzer revealed some degradation of the charge collection in the pixel border regions. To examine this effect, a 2 mm diameter collimated ^{55}Fe source was placed directly at the center of pixel #4 (a larger collimator was used in order to obtain improved statistics). PHA spectra from pixel #4 were recorded (T_p=0.5 μs) as the source was scanned diagonally towards the center of the array where all pixels share a common border. The results shown in Fig. 5 clearly demonstrate the degradation of charge collection in the boundary region. As the source is scanned towards the array center the principal peak in the PHA spectra should decrease by a factor of four to reflect equal distribution of the photons among the four pixels. However, the experimental result is a 4.5x decrease accompanied by high-energy tailing. Depending on the span of the SCA window employed as a discriminator, a finite percentage of the photons would be uncounted. For example using a 700 eV window, ~20% of the photons falling within 1 mm of the pixel borders would not be counted. This translates into two segments of dead volume each of which is represented by 20% of a 2 x 20 mm rectangular area. Under these conditions, the uppermost limit of the inactive volume of the array is estimated at 2%. This contrasts to other detector designs that have inactive volumes of 10-50%.[3-5] The solid angle that the spectrometer intercepts is 25% of 2π sr when originating from a point source at a distance of 1 cm. Although the subtended solid angle is smaller than those of other multi-element detectors, differences in the respective dead volumes and fluorescence photon path lengths to the pixels make the monolithic design equivalent to or better in terms of photon collection.

The fluorescence detector system has been used for several successful XAS investigations including low level near edge and EXAFS measurements of various actinide materials at the L_{III} edge. The detector system has also been employed at photon energies other than those associated

with actinides, to ascertain its suitability for more general use. Fluorescence measurements at the Ce L_{III} and Cs K edges (5.7 and 36 keV, respectively) have been performed and demonstrate that the detector system performs well at these photon energies. An integral shield for the detector nose cone barrel was fabricated to reduce contributions from unwanted scattered radiation. The detector is kept at LN_2 temperatures at all times. Specialized high voltage ramp electronics, built at LBNL, provides protection for the pixel contacts by limiting the rate at which voltage may be applied or discharged from the detector element.

IV. CONCLUSION

The performance of this detector system represents an improvement over existing multi-element Ge detector systems in terms of the maximum count rate available per pixel. The operation of the detector system is straightforward and after a full year of use the pixel characteristics are indistinguishable from the initial values. Full implementation of dead time corrections will allow for utilization of even larger ICR rates per pixel. Further gains in both resolution and throughput will be accomplished when higher performance FET's are installed in the near future and faster circuits are incorporated in each channel of detector electronics. Future detectors based on this monolithic design may prove to be desirable solutions for many SR detection requirements on a cost effective basis.

ACKNOWLEDGMENTS

This work was supported in by the Director, Office of Energy Research, Office of Basic Energy Sciences, Chemical Sciences Division of the U. S. Department of Energy under Contract No. DE-AC03-76SF00098. This work was performed in part at SSRL which is funded by the Department of Energy, Office of Basic Energy Sciences., Chemical Sciences Division. The authors thank M. Press, J. Zaninovich, and J. Katz of the LBNL Engineering Division for the fabrication of the high voltage electronics.

REFERENCES

1. J. Jaklevic, J. A. Kirby, M. P. Klein, A. S. Robertson, G. S. Brown, and P. Eisenberger, Solid State Commun. **23**, 679 (1977).
2. S. P. Cramer, O. Tench, M. Yocum, and G. N. George, Nucl. Instr. and Meth. **A266**, 586 (1988).
3. G. E. Derbyshire, A. J. Dent, B. R Dobson, R. C. Farrow, A. Felton, G. N. Greaves, C. Morrell, and M. P. Wells, Rev. Sci. Instr. **63**, 814 (1992).
4. L. R. Furenlid, H. W. Kraner, L. C. Rogers, S. P. Cramer, D. Stephani, R. H. Beuttenmuller, and J. Beren, Nucl. Instr. and Meth. **A319**, 408 (1992).
5. J. S. Iwanczyk, N. Dorri, M. Wang, R. W. Szczebiot, A .J. Dabrowski, B. Hedman, K. O. Hodgson, and B. E. Patt, IEEE Trans. Nucl. Sci. **39**, 1275 (1992).
6. J. J. Bucher, P. G. Allen, N. M. Edelstein, and D. K. Shuh (unpublished).
7. L. Soderholm and M. Antonio (to be published).

FIGURE CAPTIONS

1. Schematic of the monolithic semiconductor element indicating the assignment of the respective pixels.
2. Detector saturation curves measured with ^{55}Fe sealed source as a function of peaking times (T_p). The resolution of the detector for each ICR is shown next to the T_p. The SCA window is wide open for the measurements.
3. Detector saturation curves collected with a ^{238}Pu sealed source as a function of peaking times (T_p). The resolution of the detector for each ICR is shown next to the T_p. The SCA window is wide open for the measurements.
4. Spatial response of the monolithic pixels determined with an ^{55}Fe sealed source collimated to 0.1 mm for 6 mm and operating at a distance of 2 mm from the detector nose cone. The solid traces are the transitions between pixels #2-1 with the thick solid line representing the performance of pixel #2. The dashed lines are the horizontal transition between pixel #2-3 with the finely dashed line identifying the response of pixel #2.
5. Comparison of PHA spectra as the ^{55}Fe source is moved from the center of pixel #4 towards the center of the Ge element. The large peak was collected from the center of pixel #4, whereas the smaller peak originates from the common center shared by all pixels. In theory, the small feature should be a factor of four less than the large feature.

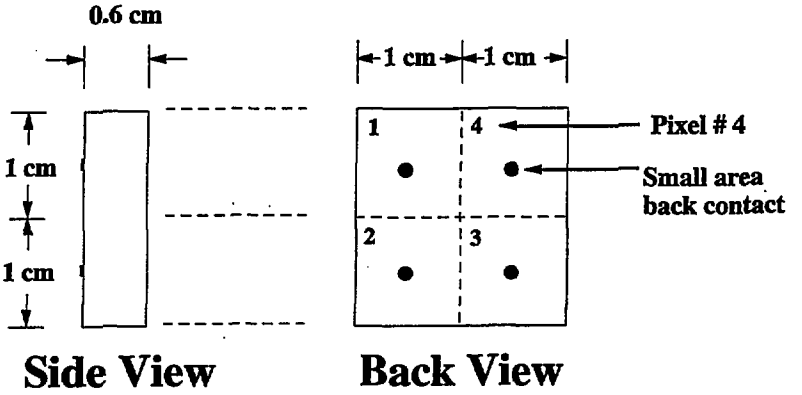

J.S. Bucher A06

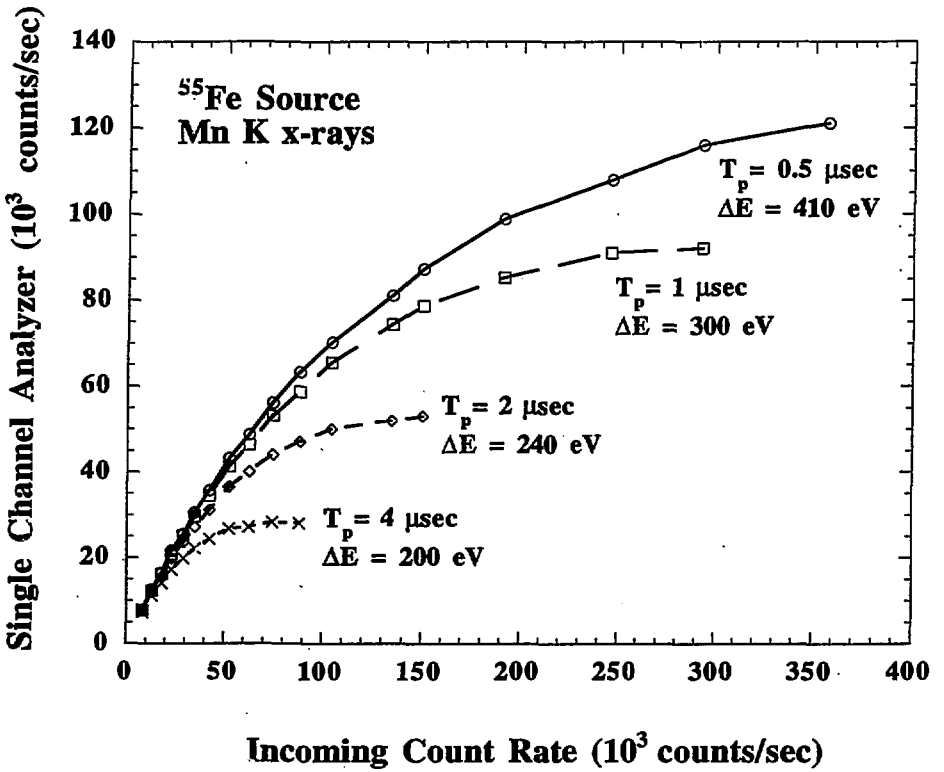

J.J. Buchhar ADG

Figure 2.

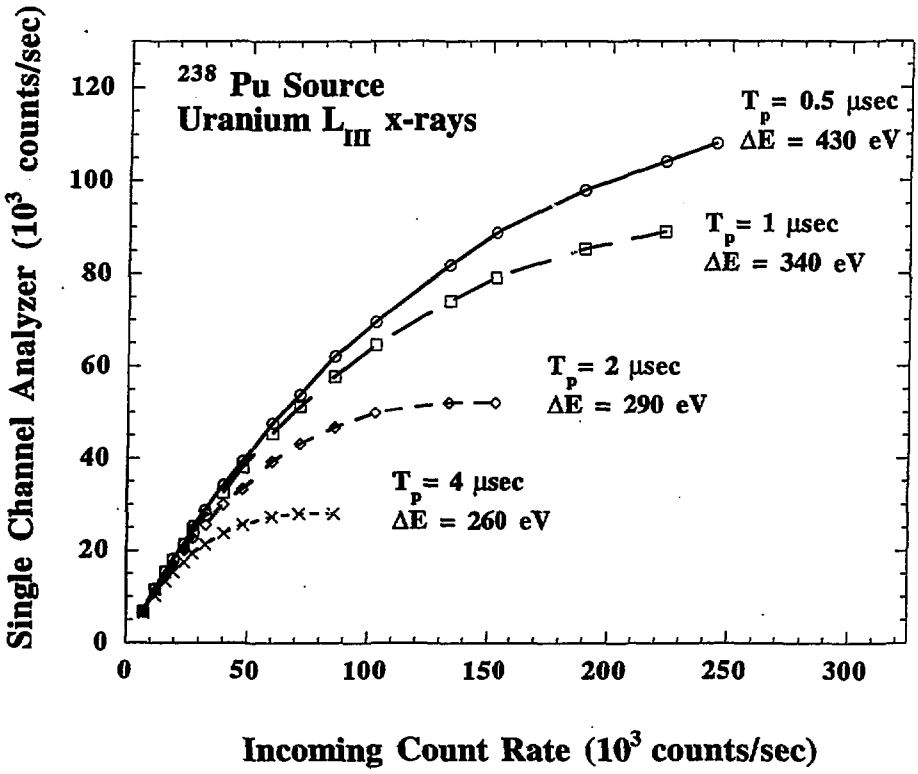

J.J. Bucher ADL

Page 3

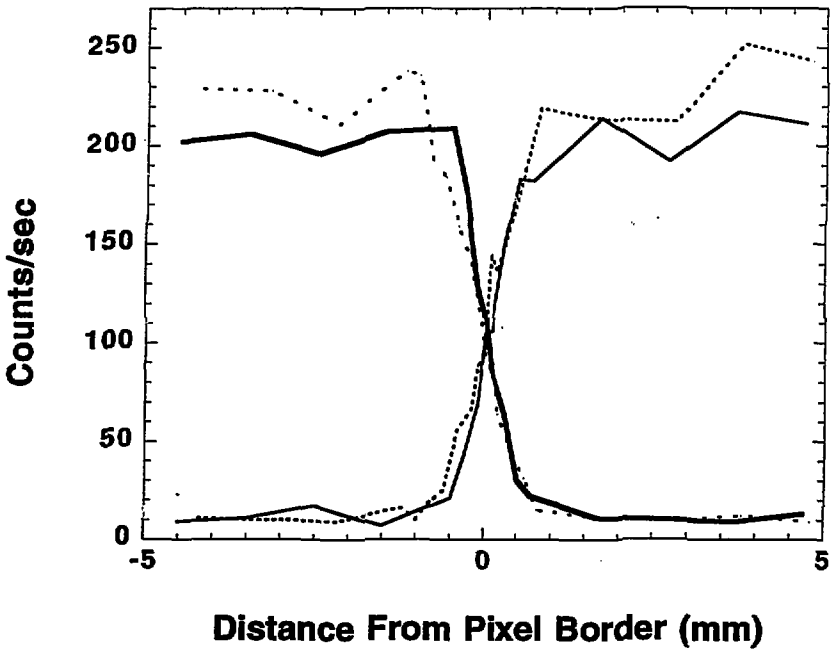

J.J. BUCHER A/C

FIG. 4

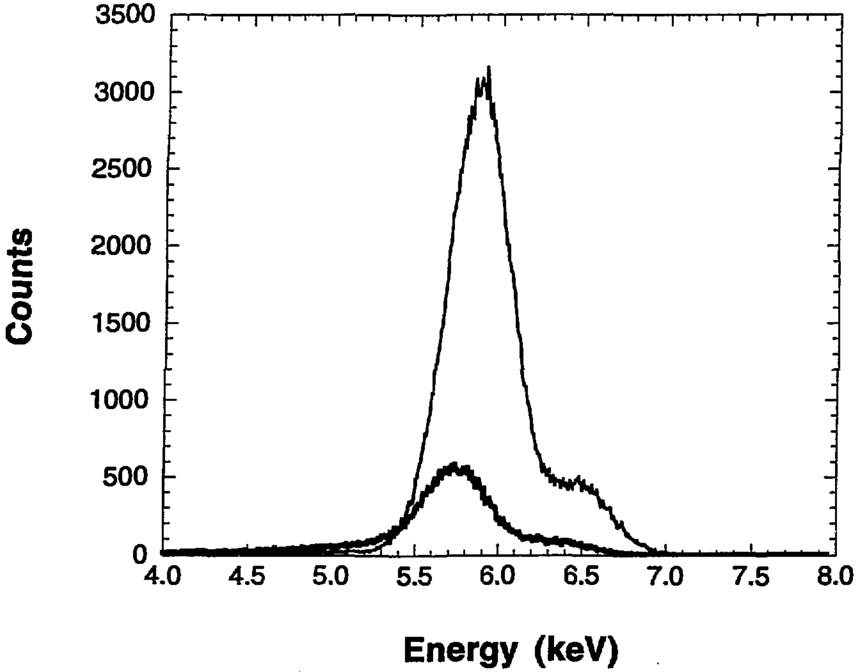

J.J. BUCHER A006

FIGURE 6